0026-895X/10/7705-773–783$20.00
MOLECULAR PHARMACOLOGY
Vol. 77, No. 5
62497/3580696
Mol Pharmacol 77:773–783, 2010
Printed in U.S.A.

Identification of Stage-Specific Gene Modulation during Early Thymocyte Development by Whole-Genome Profiling Analysis after Aryl Hydrocarbon Receptor Activation

Michael D. Laiosa, Jeffrey H. Mills, Zhi-Wei Lai, Kameshwar P. Singh, Frank A. Middleton, Thomas A. Gasiewicz, and Allen E. Silverstone

Department of Environmental Medicine, University of Rochester, Rochester, New York (M.D.L., K.P.S., T.A.G.); and the Departments of Microbiology and Immunology (J.H.M., Z.W.L., A.E.S.) and Neuroscience and Physiology (F.A.M.), State University of New York, Upstate Medical University, Syracuse, New York

Received November 17, 2009; accepted February 12, 2010

ABSTRACT

The aryl hydrocarbon receptor (AHR) is a basic helix-loop-helix transcription factor, implicated as an important modulator of the immune system and of early thymocyte development. We have shown previously that AHR activation by the environmental contaminant and potent AHR agonist 2,3,7,8-tetrachlorodibenzo-*p*-dioxin (TCDD) leads to a significant decline in the percentage of S-phase cells in the $CD3^-CD4^-CD8^-$ triple-negative stage (TN) 3 and TN4 T-cell committed thymocytes 9 to 12 h after exposure. In the more immature TN1- or TN2-stage cells, no effect on cell cycle was observed. To identify early molecular targets, which could provide insight into how the AHR acts as a modulator of thymocyte development and cell cycle regulation, we performed gene-profiling experiments using RNA isolated from four intrathymic progenitor populations in which the AHR was activated for 6 or 12 h. This microarray analysis of AHR activation identified 108 distinct gene probes that were significantly modulated in the TN1–4 thymocyte progenitor stages. Although most of the genes identified have specific AHR recognition sequences, only seven genes were altered exclusively in the two T-cell committed stages of early thymocyte development (TN3 and TN4) in which the decline of S-phase cells is seen. Moreover, all seven of these genes were reduced in expression, and five of the seven are associated with cell cycle regulatory processes. These seven genes are novel targets for modulation by the TCDD-activated AHR and may be involved in the observed cell-cycle arrest and suppression of early thymocyte development.

The aryl hydrocarbon receptor (AHR), a member of the basic helix loop helix–periodicity/aryl hydrocarbon receptor nuclear translocator/single-minded (PAS) family of transcription factors, has been implicated as an important modulator of immune system development and function (Stevens et al., 2009; Stockinger et al., 2009). Studies using AHR-null mice suggest that AHR-dependent gene transactivation is required for normal vascular development, circadian rhythms, and hematopoietic stem cell regulation (Fernandez-Salguero et al., 1996; Schmidt et al., 1996; Garrett and Gasiewicz, 2006). AHR agonists regulate tolerogenic signaling in autoimmunity models, cause immune suppression in infectious disease models, and modulate cell cycle regulation during early thymocyte development (Laiosa et al., 2003; Funatake et al., 2005; Hogaboam et al., 2008; Quintana et al., 2008; Veldhoen et al., 2008).

Given the requirement for the thymus in establishing central tolerance, we have had an interest in identifying the molecular mechanisms by which AHR-dependent gene modulation within thymocyte progenitors modulates cell cycle regulation in specific stages of thymocyte ontogeny. We have shown previously that AHR activation by TCDD causes a dramatic reduction in cell cycle progression within 9 to 12 h of in vivo exposure to TCDD within a subset of cells called TN3 and TN4 but not in their immediate thymocyte precursors TN1 and TN2 (Laiosa et al., 2003). Identification of the stage TN3 and TN4 thymocytes

This work was supported by the National Institutes of Health National Institute of Environmental Health Sciences [Grants K99-ES016585, R01-ES04862, ES07026, ES01247].

Article, publication date, and citation information can be found at http://molpharm.aspetjournals.org.

doi:10.1124/mol.109.062497.

ABBREVIATIONS: AHR, aryl hydrocarbon receptor; TCDD, 2,3,7,8-tetrachlorodibenzo-*p*-dioxin; TN, triple negative; TCRβ, T-cell antigen receptor β; ANOVA, analysis of variance; IPA, ingenuity pathway assist; MTAP, 5-methythioadenosine phosphorylase; RT^2-PCR, real-time reverse transcriptase PCR.

as proximal targets of AHR activation is important because the TN3–TN4 developmental transition is a critical checkpoint during thymocyte development at which the *T-cell antigen receptor β (TCRβ)* gene locus is rearranged. The resulting protein is trafficked to the cell surface in a complex known as the pre-TCR. If the pre-TCR is functional, the cell becomes committed to the αβ-T-lineage, the TCRβ rearrangement machinery is turned off, and cell survival is driven by pre-TCR–dependent signals. Pre-TCR–dependent survival signals drive entry into the cell cycle, lead to differentiation into TN4 stage cells, and make possible the eventual up-regulation of the CD4 and CD8 TCR coreceptors. There are some important questions that remain from this earlier work: how does AHR-dependent signal transduction modulate cell cycle in the pre-TCR–dependent stage of T cell development? Is it caused by direct modulation of cell cycle regulating genes expressed in the TN3 and TN4 subsets, indirectly through modulation of other immune-specific growth-regulatory genes, or are other unique gene-regulatory pathways modulated by the AHR in these cells that affect cell-cycle progression and thymocyte maturation?

To begin to address the mechanism by which AHR activation effects cell proliferation and thymocyte differentiation, we conducted gene-profiling experiments to identify candidate genes and gene pathways modulated specifically in the TN1 through TN4 stages of early thymocyte development. Our approach is distinct from previous gene profiling investigations, which focused on either whole thymus preparations or on a single population of cells within the thymus (Svensson and Lundberg, 2001; McMillan et al., 2007). For example, the gelsolin-like protein scinderin (adseverin 5) was identified as a thymus-specific marker induced by TCDD activation of AHR in all thymocyte subsets, including stages TN1 through TN4 (Svensson et al., 2002). In another study, genes associated with the KLF2 regulon were modulated by AHR activation by TCDD in a thymocyte population not seen in normal mice (McMillan et al., 2007). However, these investigators used a higher dose of TCDD than in most previous studies, and they also conducted their in vivo studies in mice deficient for the recombinase activating gene-2 (McMillan et al., 2007); these mice have a complete block in thymocyte development at stage TN3 owing to their inability to rearrange the *T-cell antigen receptor β* locus and inability to express a functional pre-TCR (Mombaerts et al., 1992; Levelt et al., 1993). Consequently, the gene expression changes observed in this study may be secondary to the aborted pre-TCR–dependent survival signaling in these mice.

Our genetic profiling approach differed from these earlier studies because it did not bias the results using genetically modified mice, a preselected cell population, or extracts from the entire heterogeneous mixture of thymocytes. To determine the actual early gene regulation events modulated by an activated AHR that could explain the cell cycle effects in the pre-TCR stage of thymocyte development, we performed 16 separate gene-profiling experiments using RNA obtained from sorted pooled TN1 and TN2 cells, TN3, TN4A, and TN4B subsets at 6 and 12 h after exposure (Fig. 1). Gene expression changes between

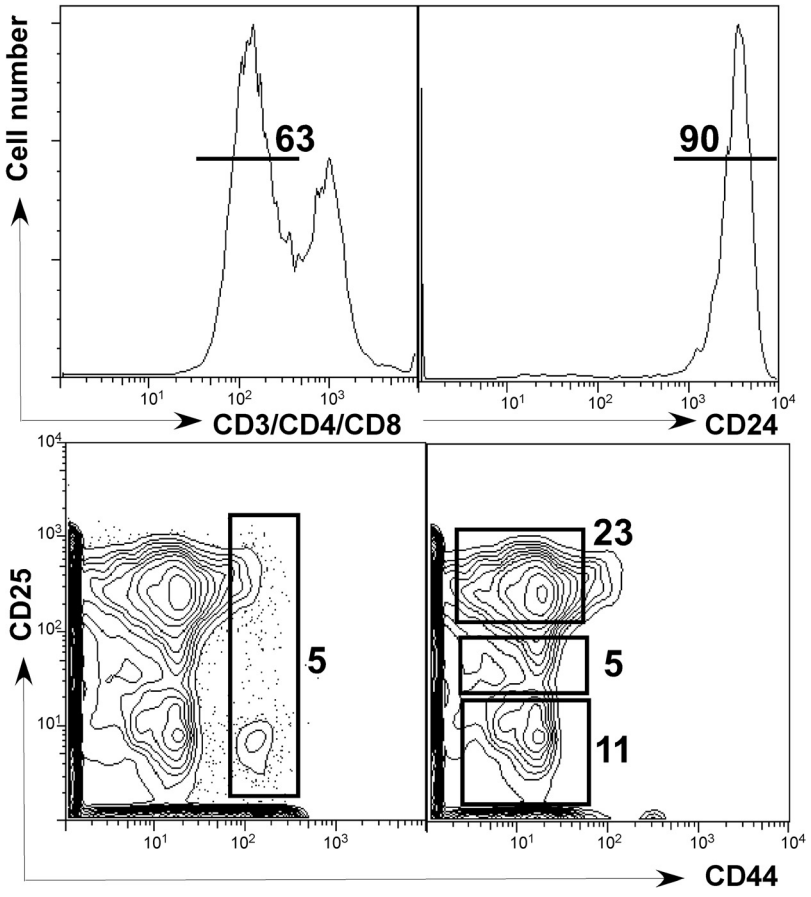

Fig. 1. Cell-sorting gates used for purifying early thymocyte progenitor populations. TN cells were identified by the absence of CD3/CD4/CD8 (top left) and then TN1+2 cells were sorted based on the expression of $CD44^{+}CD25^{+}$ (bottom left). For the TN3, TN4A, and TN4B cells, TN cells were further identified based on high expression of CD24 (top right), and then separated based on CD25 levels ($CD25^{hi}$, TN3; $CD25^{intermediate}$, TN4A; and $CD25^{lo}$, TN4B; bottom right). The frequencies of gated cells are denoted adjacent to each population. Flow cytometric sorting gate is a control sample representative of two independent experiments. There was no difference in cell distribution among the populations with TCDD at either of the two time points.

treatment, thymocyte population, and time were compared, yielding potential insights into how persistent AHR activation modulates cell cycle regulation during early thymocyte development.

Materials and Methods

Mice and Treatment Protocol. Four- to five-week-old C57BL/6J ($AHR^{b/b}$) mice were purchased from The Jackson Laboratory (Bar Harbor, ME) and allowed to acclimate for 1 full week after arrival at the Upstate Medical University. Mice were maintained on a 12-h dark/light cycle and were provided food (5001 rodent diet; Purina Mills, St. Louis, MO) and water ad libitum. All mice were housed and cared for according to protocols approved by the animal welfare committees at both the State University of New York Upstate Medical University and the University of Rochester.

TCDD was obtained from Cambridge Isotopes (Andover, MA). A stock solution in the solvent *p*-dioxane (Sigma-Aldrich, Milwaukee, WI) was diluted to an appropriate concentration in olive oil (F. Berio, Lucca, Italy) to yield a treatment solution containing 6 μg/ml TCDD. Either 30 μg/kg TCDD in olive oil/kg body weight or olive oil alone in a volume of 0.1 ml/20 g body weight was intraperitoneally injected into mice 6 or 12 h before euthanasia. Injections were scheduled such that euthanasia and tissue harvest could be completed for one group of five mice before the second group was started (1 h apart). Thymocytes were pooled from five mice per group, and each time point was conducted four times for TCDD and four times for control.

Flow Cytometry Staining and Cell Sorting. Mice were euthanized by CO_2 asphyxiation, followed by cervical dislocation at the appropriate time point after TCDD exposure. For each experimental group, thymi from five mice were removed and pooled, and cell suspensions were made in ice-cold MEM containing 5% fetal bovine serum plus 100 U/ml penicillin and 0.1 mg/ml streptomycin (Invitrogen, Carlsbad, CA). Debris was eliminated by passing the cell suspension through Pasteur pipettes containing 80-gauge nylon mesh (Tetko, Kansas City, MO). Cell yield and viability were enumerated with a Neubauer hemocytometer (Reichert, Buffalo, NY). Cell viability was determined to be >95% from all cell suspensions by trypan blue dye exclusion.

Pooled thymocytes were washed with phosphate-buffered saline, 0.5% bovine serum albumin, and 0.1% sodium azide in preparation for enrichment of CD4 negative cells. Specifically, thymocytes were labeled with magnetic microbead-conjugated anti-CD4 (clone RM4–5, rat immunoglobulin G2a) (BD Biosciences, San Jose, CA) according to the manufacturer's instructions. After labeling was complete, cells were washed, resuspended in running buffer (phosphate-buffered saline, 0.5% bovine serum albumin, and 0.1% sodium azide), and separated using the EasySep magnet (Stem Cell Technologies, Vancouver, BC, Canada). Enriched cells were counted and prepared for fluorochrome labeling and fluorescence-activated cell sorting.

In preparation for cell sorting, CD4 negative thymocytes were CD16/CD32-blocked (clone 2.4G2) and subsequently stained with a cocktail of phycoerythrin-Texas Red conjugated CD3 (clone 145-2C11), CD4 (clone L3T4), CD8 (clone 53-6.7), $\alpha\beta$ TCR (clone H57-597), $\gamma\delta$ TCR (clone GL-3), CD11b (clone M1/70), CD11c (clone HL3), GR-1 (clone RB6-8C5), NK1.1 (clone PK136), B220 (clone RA3–6B2), and Ter119. In addition, cells were stained with phycoerythrin-conjugated CD24 (heat stable antigen; clone M1/69), FITC- conjugated CD25 (clone 7D4), and APC-conjugated CD44 (clone IM7). All antibodies were purchased from BD Biosciences (San Jose, CA). After TN-enriched thymocytes were labeled with fluorescence-conjugated antibodies directed at thymocyte surface antigens, cells were separated into four triple-negative (TN) populations designated TN1+2, TN3, TN4A, and TN4B with the use of a BD FACSVantage cell sorter and BD FACSDiva software version 5.

Microarray Studies. To evaluate the molecular mechanisms underlying effects of AHR activation on thymocyte differentiation after TCDD exposure, we performed comprehensive gene expression profiling with the mouse 430 2.0 GeneChip (Affymetrix, Santa Clara, CA). RNA for these analyses was obtained from three independent replicate preparations involving four FACS-sorted fractions (TN1+2, TN3, TN4A, TN4B) at two time points (6 and 12 h) after exposure to either TCDD or vehicle. Thus, 48 RNA samples (three replicates $\times$ four fractions $\times$ two time points $\times$ two treatments) were used for microarray analysis. The RNA from these preparations was purified using the RNeasy kit (QIAGEN, Valencia, CA), and the quality and yield were examined using the RNA NanoChip (Agilent Technologies, Santa Clara, CA). Amplification and labeling of the 48 RNA samples was performed using the WT-Ovation RNA Amplification System (NuGen, San Carlos, CA), and processing of the GeneChips was performed according to standard protocol (GeneChip Expression Analysis Technical Manual 701021 rev 5; Affymetrix). After scanning, the microarray images were analyzed using GeneChip Operating System software to obtain performance metrics, and normalized using the robust multiarray average method during import into GeneSpring GX 9.0 (Agilent).

Significant differences in transcript expression were determined using a three-way analysis of variance (ANOVA) comparing treatment $\times$ fraction $\times$ time ($2 \times 4 \times 2$ ANOVA). The nominal significance for the main effect that was obtained was adjusted for multiple testing of the 45,101 probes on the 430 2.0 array using the Bonferroni-Holm method (with $\alpha = 0.05$). Because our primary aim in this report was to determine those genes with significant TCDD-induced expression changes, we focused our analysis on those probes with a significant main effect of treatment and/or a significant interaction of treatment and time after correction ($n = 108$ total probes).

IPA Functional Analysis. To further understand the biological relevance of the statistically significantly changed probes, we used ingenuity pathway assist (IPA) to explore their relationships and known annotations. Enrichment scores and/or *P* values were automatically generated by the software for the top implicated functional networks, bio functions, and canonical pathways based on a comparison of the uploaded 108 probes compared with the annotated content of the 430 2.0 GeneChip.

TABLE 1

Stage-specific analysis of mRNA expression for developmentally regulated thymocyte genes demonstrates transcriptional purity of the cell sorting and confirms selected microarray data

Thymocyte progenitors were sorted into individual TN1–TN4 sub-populations, RNA extracted and purified and RT^2-PCR performed using primers specific for developmentally regulated transcripts within early thymocyte progenitor populations. Relative fold difference was determined by dividing the expression levels of the gene from the enriched or deficient population (listed in the left column) by the expression level of the same gene in the population shown in the top column. Genes selected for RT^2-PCR analysis were: CD44, CD8α, and Ptcra (Pre-TCRα).

Thymocyte Subset	Relative Fold Changes in Selected Progenitor Populations			
	TN1+2	TN3	TN4A	TN4B
TN1+2-enriched genes with reduced relative expression in other subsets	CD44	0.03	0.02	0.03
TN1+2-deficient genes with elevated relative expression in other subsets	Ptcra	31.0	5.8	5.3
	CD8		15.9	23.0
TN3-deficient genes with elevated relative expression in other subsets		CD8	12.6	18.3

TABLE 2

Gene profiling 6 to 12 h of AHR activation in thymocyte progenitors results in 108 significantly modulated gene probes

Results determined by Bonferroni-Holm correction and three-way ANOVA reporting a significant main effect with treatment, and/or significant interaction of treatment and time. The mean fold induction across all four sorted populations from TCDD-exposed mice is shown at 6 and 12 h.

Unigene (Avadis)	Gene Symbol	Gene Title	Mean Fold Change	
			6-h TCDD	12-h TCDD
Mm0.372315	*1700097N02Rik*	RIKEN cDNA 1700097N02 gene	1.2	1.1
Mm0.273197	*2010002N04Rik*	RIKEN cDNA 2010002N04 gene	−1.0	−1.7
Mm0.131555	*A630007B06Rik /// LOC674488*	Similar to oocyte-testis gene 1	−1.0	−1.5
Mm0.19941	*Acpp*	Acid phosphatase, prostate	1.2	1.4
Mm0.291826	*Adipor2*	Adiponectin receptor 2	1.1	1.4
Mm0.290446	*Ahrr*	Aryl-hydrocarbon receptor repressor	1.1	4.3
Mm0.23125	*AI425999*	Expressed sequence AI425999	1.7	1.7
Mm0.42040	*Ak3l1 /// LOC100047616*	Adenylate kinase 3 α-like 1	−1.0	−1.8
Mm0.36006	*Ak7*	Adenylate kinase 7	1.5	1.1
Mm0.398221	*Aldh3a2*	Aldehyde dehydrogenase family 3, subfamily A2	−1.0	−1.5
Mm0.291372	*Arhgap8*	Rho GTPase-activating protein 8	−1.2	−3.3
Mm0.380514	*AW061096*	Expressed sequence AW061096	−1.0	−1.7
Mm0.306720	*C4bp*	Complement component 4 binding protein	1.2	1.5
Mm0.10702	*Cacybp*	Calcyclin binding protein	−1.1	−1.1
Mm0.25457	*Ccno*	Cyclin O	1.5	2.4
Mm0.440604	*Ccr9*	Chemokine (C-C motif) receptor 9	1.4	1.1
Mm0.29204	*Cd96*	CD96 antigen	1.2	−1.7
Mm0.1135	*Cpa3*	Carboxypeptidase A3, mast cell	−1.1	−1.5
Mm0.930	*Ctsl*	Cathepsin L	−1.2	−2.4
Mm0.14089	*Cyp1a1*	Cytochrome P450, family 1, subfamily a, polypeptide 1	1.4	5.2
Mm0.214016	*Cyp1b1*	Cytochrome P450, family 1, subfamily b, polypeptide 1	2.6	14.1
Mm0.60526	*Dmn*	Desmuslin	1.1	2.4
Mm0.461605	*E430022K19Rik*	RIKEN cDNA E430022K19 gene	3.0	1.3
Mm0.379893	*EG545216 /// Glcci1 /// LOC100046012*	Glucocorticoid induced transcript 1	1.5	1.4
Mm0.296317	*EG624866*	Predicted gene, EG624866	1.1	1.8
Mm0.38929	*Esm1 /// LOC632677*	Endothelial cell-specific molecule 1	−1.3	−1.4
Mm0.261859	*Exoc3*	Exocyst complex component 3	−1.5	−1.9
Mm0.28095	*Flnb*	Filamin, β	−1.1	−3.6
Mm0.11982	*Gas2l3*	Growth arrest-specific 2 like 3	1.6	1.0
Mm0.210787	*Glcci1*	Glucocorticoid induced transcript 1	1.1	1.5
Mm0.245741	*Heg1*	HEG homolog 1 (zebrafish)	3.2	1.6
Mm0.57250	*Hic1*	Hypermethylated in cancer 1	1.0	1.6
Mm0.239865	*Hspa4*	Heat shock protein 4	1.0	1.2
Mm0.209419	*Hspa9*	Heat shock protein 9	−1.1	−1.0
Mm0.106343	*Ikzf2*	IKAROS family zinc finger 2	1.4	1.1
Mm0.731	*Il12rb1*	Interleukin 12 receptor, β1	1.0	1.6
Mm0.389	*Il7r*	Interleukin 7 receptor	−1.2	−1.1
Mm0.58	*Itgb7*	Integrin β7	−2.2	−3.1
Mm0.228812	*Jakmip1*	Janus kinase and microtubule interacting protein 1	1.4	1.1
Mm0.26938	*Klf2*	Kruppel-like factor 2 (lung)	−1.9	−3.9
Mm0.248615	*Lgals3*	Lectin, galactose binding, soluble 3	−1.0	−31.9
Mm0.33240	*Mpzl2*	Myelin protein zero-like 2	1.4	1.1
Mm0.28500	*Mtap*	Methylthioadenosine phosphorylase	1.0	1.2
Mm0.275281	*Narg1*	*N*-methyl-D-aspartate receptor-regulated gene 1	−1.2	−1.1
Mm0.170515	*Nfkbia*	Nuclear factor of κ light chain gene enhancer in B cells inhibitor, α	1.2	1.0
Mm0.220367	*Nol5*	Nucleolar protein 5	1.2	1.2
Mm0.402190	*Nolc1*	Nucleolar and coiled-body phosphoprotein 1	1.0	1.3
Mm0.2380	*Npas2*	Neuronal PAS domain protein 2	2.3	2.6
Mm0.252	*Nqo1*	NAD(P)H dehydrogenase, quinone 1	1.2	2.1
Mm0.423531	*Nrp1*	Neuropilin 1	−1.1	−1.2
Mm0.3304	*Nsg2*	Neuron specific gene family member 2	−1.1	−1.5
Mm0.390681	*P2ry5*	Purinergic receptor P2Y, G-protein coupled, 5	1.4	1.9
Mm0.259103	*Phc2*	Polyhomeotic-like 2 (*Drosophila melanogaster*)	−1.5	−2.4
Mm0.253819	*Pik3r3*	Phosphatidylinositol 3 kinase, regulatory subunit, polypeptide 3 (p55)	−1.1	−2.7
Mm0.192699	*Plcg2*	Phospholipase C, γ2	−1.2	−2.5
Mm0.897	*Pou2af1*	POU domain, class 2, associating factor 1	−1.1	−1.8
Mm0.70065	*Ppm1 h*	Protein phosphatase 1H (PP2C domain containing)	1.1	1.2
Mm0.2415	*Pprc1*	Peroxisome proliferative activated receptor, γ, coactivator-related 1	−1.2	−1.3
Mm0.379451	*Pqlc3*	PQ loop repeat containing	1.1	2.0
Mm0.27705	*Prim2*	DNA primase, p58 subunit	1.3	1.2
Mm0.16766	*Prkacb*	Protein kinase, cAMP dependent, catalytic, β	1.2	1.2
Mm0.381172	*Prkg1*	Protein kinase, cGMP-dependent, type I	1.2	1.9
Mm0.103522	*Pwp2*	PWP2 periodic tryptophan protein homolog (yeast)	−1.1	−1.4
Mm0.196846	*Rad23b*	RAD23b homolog (*Saccaromyces cerevisiae*)	1.3	1.1
Mm0.42150	*Rasgrp1*	RAS guanyl releasing protein 1	1.0	1.2

continued

Real-Time Quantitative Reverse Transcription-PCR Validation. From the list of genes with significant changes in expression as a result of treatment, as well as genes known to be differentially expressed in specific fractions, we derived a set of eight genes to use for validation of the microarray findings [*Acpp* (acid phosphatase, prostate), *CD44*, *CD8a*, *Cyp1b1*, *PtcrA* (pre-TCRa), *Scin* (Scinderin), *Tparp* (TCDD-inducible poly(ADP-ribose) polymerase), and *Trpm1*]. Primers for each of these genes were obtained from previous reports or custom-designed using Primer3 software. Once the optimal conditions were obtained for each primer set, the quantification reactions were performed on the same RNA fractions prepared for the microarrays. Thermal cycling was performed on an iCycler iQ5 (Bio-Rad Laboratories, Hercules, CA) in triplicate reactions on 96-well plates. Ribosomal protein S6 (Rps6) was chosen as the internal reference gene, and differences in expression were calculated using the ΔC_t method. Statistical significance was determined using a repeated measures ANOVA on all 10 genes, with a Scheffé post hoc test.

Results

Thymocyte Cell Numbers Are Unchanged by TCDD Exposure. To identify the AHR-dependent modulation of gene expression that potentially mediates alterations in early thymocyte cell cycle regulation and T-cell development, we sorted early-stage thymocytes from vehicle- or TCDD-exposed mice, extracted RNA from each pool of cells, and performed a gene profiling experiment on the RNA from each stage of early thymocyte development. As shown in Fig. 1, the sorting gates chosen were designated TN1+2, TN3, TN4A, and TN4B. It is noteworthy that there were no differences in frequency among the four populations between vehicle or TCDD-exposed groups at either time point (data not shown; Laiosa et al., 2003).

The sorting gates shown in Fig. 1 separate the thymocyte progenitors four ways consisting of a pooled TN1+2 population and the three T-committed populations: TN3, TN4A, and TN4B to identify gene expression changes in each subset dependent on AHR activation. Cell sorting based on CD44, CD25, and CD24 resulted in populations that were at least 98% pure.

As further confirmation of purity, reverse transcription-PCR was performed on RNA isolated from each population using genes known to be differentially expressed during early thymocyte development. Specifically, the gene expression patterns of CD44, preTα (Ptcra), and CD8 were analyzed in each sorted population to confirm that CD44 expression is enriched in the TN1+2 subset, preTα is enriched in the TN3 (with lower expression in TN4), and CD8 expression is relegated to TN4A and TN4B. Indeed, as shown in Table 1, expression levels of the developmentally regulated genes were considerably higher in the appropriate stages compared with the same message levels in developmental stages, where expression is predicted to be extinguished. It is noteworthy that CD44 gene expression in the TN1+2 population was almost completely absent in the TN3, TN4A, and TN4B populations. Furthermore, the gene encoding the invariant preTα (Ptcra) was 31-fold higher in TN3 than in TN1+2. Finally, CD8 expression in TN4A was 15.9-fold enriched compared with its expression in TN1+2, and 12.6-fold enriched compared with CD8 expression in TN3. These data demonstrate the fidelity of RNA obtained from our four-way cell sorting procedure.

One Hundred Eight Probes Are Modulated by AHR Activation and Are Developmentally Regulated in Early Thymocyte Progenitors. To identify candidate genes responsible for the profound block in DNA synthesis that occurs in the TN3 and TN4 stages of thymocyte development after exposure to TCDD, we performed gene expression profiling experiments using purified RNA from each thymocyte progenitor subset. To determine those genes with significant TCDD-induced expression changes, we focused our analysis on those probes with a significant main effect of treatment and/or a significant interaction of treatment and time after correction (n = 108 total probes). This analysis identified 108 of 45,101 probes for which a significant interaction of treatment and time was observed. Of the 108 probes significantly modulated, there are 21 duplicate probes, indicating that the gene expression of 87 unique genes and/or expressed sequence tags are modulated 6 to 12 h after expo-

TABLE 2. (*Continued*)

Unigene (Avadis)	Gene Symbol	Gene Title	Mean Fold Change	
			6-h TCDD	12-h TCDD
Mm0.465324	*Rasgrp4*	RAS guanyl releasing protein 4	−1.3	−3.4
Mm0.280068	*Rcbtb2*	Regulator of chromosome condensation (RCC1) and BTB (POZ) domain containing protein 2	1.3	1.6
Mm0.2416	*Scin*	Scinderin	1.2	4.3
Mm0.335112	*Scn4b*	Sodium channel, type IV, β	1.2	3.2
Mm0.245527	*Slc35b4*	Solute carrier family 35, member B4	−1.2	−1.5
Mm0.8575	*Sox13*	SRY-box containing gene 13	−1.9	−1.2
Mm0.260838	*St8sia1*	ST8 α-*N*-acetyl-neuraminide α-2,8-sialyltransferase 1	1.4	1.8
Mm0.198414	*Stk39*	Serine/threonine kinase 39, STE20/SPS1 homolog (yeast)	1.3	4.3
Mm0.197552	*Tgfbr1*	Transforming growth factor, β receptor I	1.4	1.1
Mm0.246767	*Thada*	Thyroid adenoma associated	−1.2	−1.6
Mm0.246398	*Tiparp*	TCDD-inducible poly(ADP-ribose) polymerase	2.2	3.6
Mm0.29431	*Tmem97*	Transmembrane protein 97	−1.9	−1.1
Mm0.436756	*Tmprss4*	Transmembrane protease, serine 4	−1.2	−3.3
Mm0.323595	*Tob2*	Transducer of ERBB2, 2	0.1	−0.25
Mm0.153272	*Tsc22d1*	TSC22 domain family, member 1	−1.3	−1.8
Mm0.130793	*Upk1b*	Uroplakin 1B	1.4	2.7
Mm0.268000	*Vim*	Vimentin	−1.6	−1.9
Mm0.281079	*Wdr12*	WD repeat domain 12	−1.1	−1.1
Mm0.210188	*Zcchc2*	Zinc finger, CCHC domain containing 2	1.3	1.1
Mm0.446560		Transcribed locus	1.2	1.2
Mm0.441872		Transcribed locus	2.1	1.1

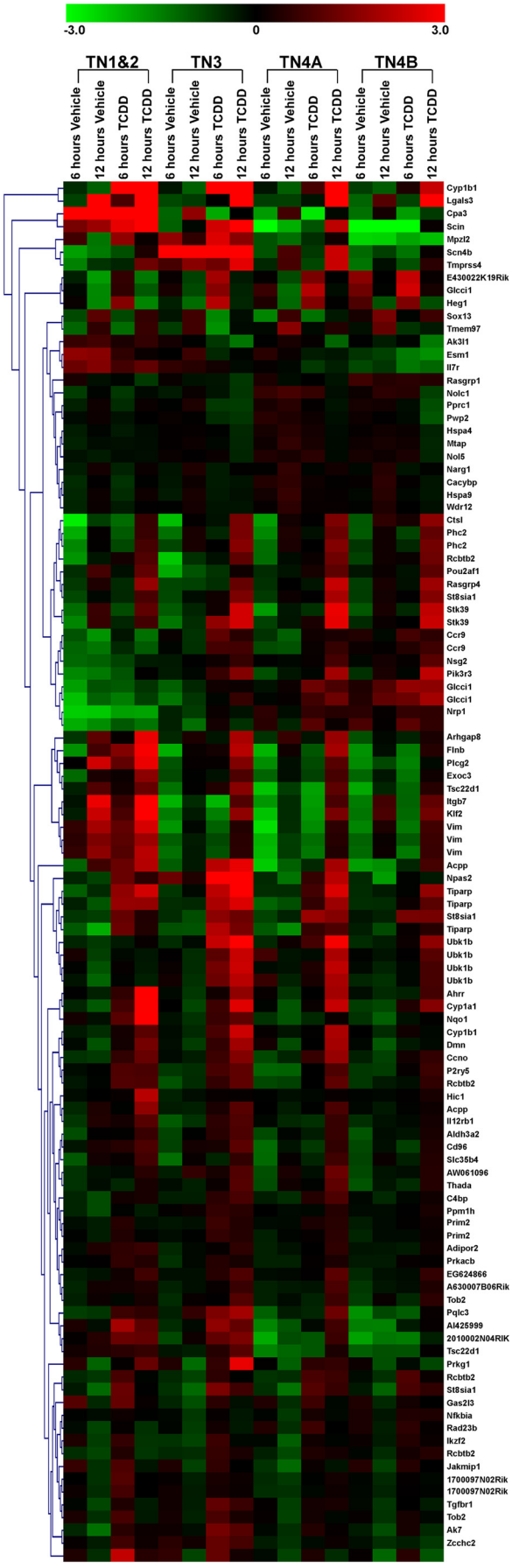

sure to TCDD compared with vehicle-exposed mice within intrathymic hematopoietic progenitor cells. The 87 genes, their symbols, and their unigene identifications are listed alphabetically in Table 2.

From the identification of the 108 gene probes demonstrating a significant interaction of treatment and time, our analysis was further refined to identify potential changes in expression, which were dependent on the stage of thymocyte differentiation. As shown in Fig. 2, a heat map was generated to display the relative expression of each of the 108 probes within each thymocyte progenitor population at 6 and 12 h after exposure to either vehicle or TCDD. Display of the relative changes for the affected probes reveals a striking diversity in responses to TCDD that is both time- and population-dependent. For example, probes corresponding to Cyp1b1, Lgals3, Ahrr, and Scin all show a significant increase in gene expression across all four populations (Fig. 2). It is noteworthy that Cyp1b1, Lgals3, Ahrr, and Scin were among the most highly TCDD-inducible probes on the array. Compared with probes found to be induced in all four sorted populations, we identified seven probes on the array that showed a significant interaction of treatment and fraction. Specifically, probes associated with Hspa4, Hspa9, Mtap, Nolc1, Pprc1, Tmem97, and Wdr12 revealed TCDD-modulated changes that occurred primarily in the TN3, TN4A, and/or TN4B populations with little to no modulation occurring in TN1+2 (Fig. 3). Moreover, the expression levels of the seven probes where gene modulation was limited to the TN3, TN4A, and/or TN4B subsets is lower after TCDD exposure compared with vehicle-treated controls. It should be noted that the identification of genes with an interaction of treatment and fraction were not selected a priori.

Validation of the results from the gene profiling experiment was performed using real-time reverse transcriptase PCR (RT^2-PCR) with primers for four genes modulated by TCDD. Specifically, Acpp, Cyp1b1, Scin, and Tparp were analyzed by RT^2-PCR for potential changes induced by TCDD in each sorted thymocyte subpopulation 6 h after exposure. As shown in Fig. 4, in each population the fold changes induced by TCDD detected by microarray were similar to the fold changes detected by RT^2-PCR. It should be noted that only genes for which a significant treatment effect of TCDD was reported are plotted. For example, the Cyp1b1 comparison is not plotted in the TN1+2 or TN4A subsets because there was not a significant treatment effect difference for Cyp1b1 in these two subsets. In addition, robust multiarray average normalization is known to underestimate true changes, particularly for low-expressing genes. This underestimation may account for the discrepancies between RT^2-PCR and microarray expression data that are observed for scinderin in the TN4A and Cyp1b1 and Tparp in the TN4B population.

IPA Functional Analysis. We explored functional relevance of 87 significantly changed genes using IPA. Results for the top five implicated functional networks, bio functions (which includes three classes: diseases and disorders, molec-

Fig. 2. Heat map of 108 gene probes significantly modulated as determined by ANOVA for treatment × fraction × time. Genes are clustered according to similar expression patterns across the four populations, and the gene name abbreviations are shown on the right side. Fold intensity scale is shown at the top of the heat map.

ular and cellular functions, and physiological system development and function), and canonical pathways are all displayed in Tables 3 to 5. Examination of these data showed that the top ranked functional network (endocrine system development and function, lipid metabolism, small molecule biochemistry) was highly similar to the second-ranked functional network. In addition, the top bio functions in the molecular and cellular function class and physiological system development and function class were also highly similar and related to fifth-ranked functional network (cell morphology, cellular development, cellular growth and proliferation; Table 4). Because of these redundancies, we elected to dis-

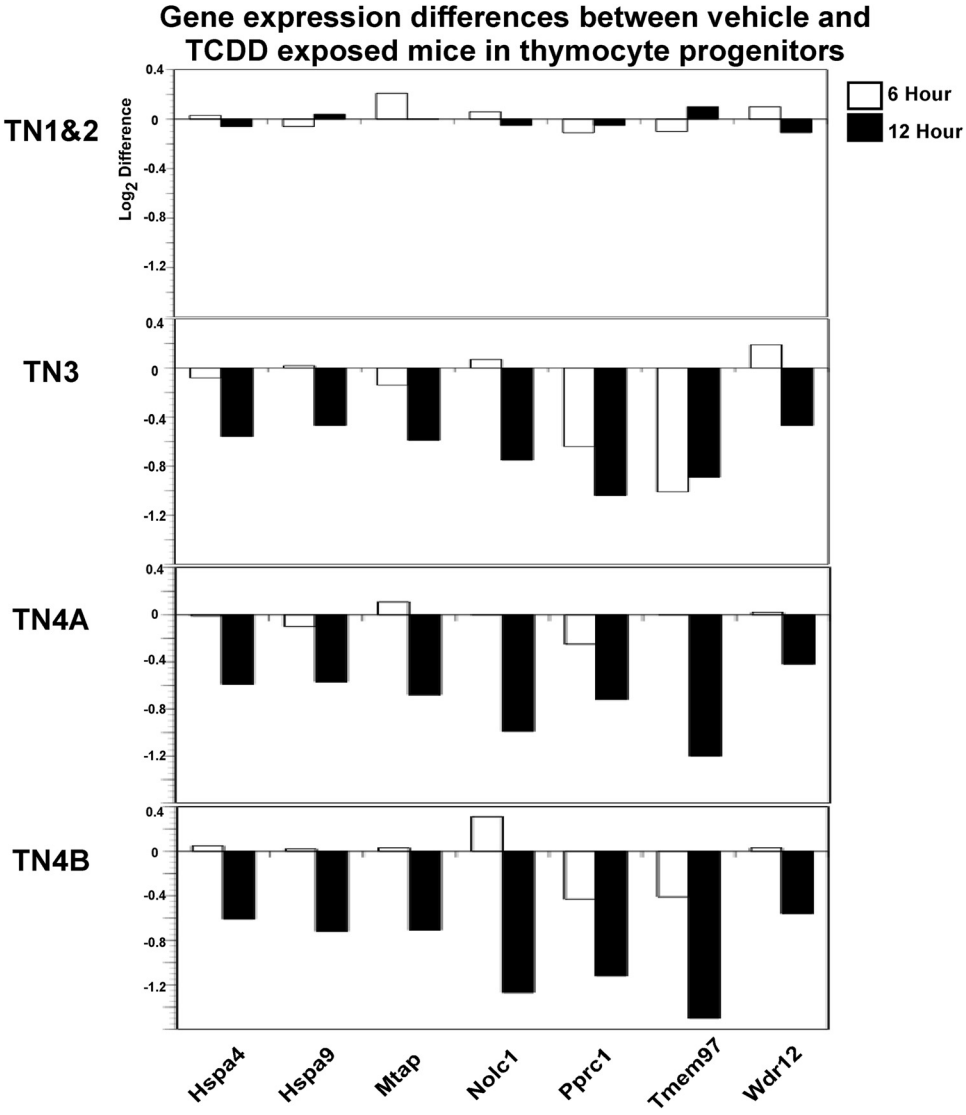

Fig. 3. Gene expression differences between control and TCDD exclusive to the T-cell-committed thymocyte progenitor populations. Seven gene probes were identified in which there was little to no difference between control and TCDD in the TN1+2 subsets but a significant difference in TN3, TN4A, and/or TN4B. The difference in probe intensity between control and TCDD is plotted for each of the seven genes at the 6- and 12-h time points.

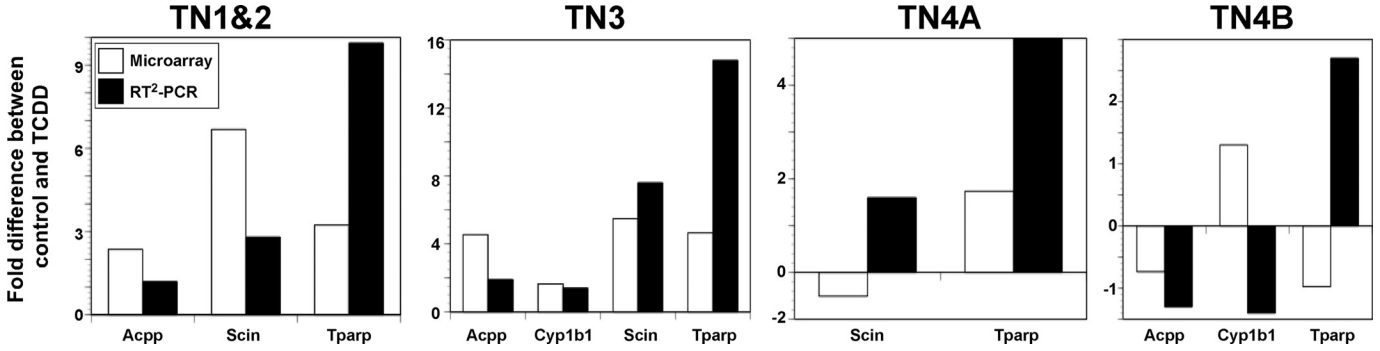

Fig. 4. Fold differences detected by RT^2-PCR are correlated to fold differences detected by microarray analysis for selected genes in each population. RT^2-PCR was performed on four known AHR-regulated genes in each population, and the fold difference between vehicle and TCDD exposure at 6 h was compared with fold differences detected by microarray. Only genes showing a significant treatment ($p \leq 0.05$) effect by RT^2-PCR analysis are compared.

play biological interaction networks for the first- and fifth-ranked functional networks (Fig. 5).

Discussion

We conducted in vivo gene profiling analysis in defined stages of early thymocyte development to identify candidate genes that could potentially explain the alterations in the development of thymocyte progenitors after AHR activation by TCDD. In TCDD-exposed mice, we identified 108 unique gene probes for which the corresponding 87 gene products were modulated, relative to vehicle-treated mice. Our rationale for analyzing gene expression within individual early thymocyte subsets was based on our earlier findings demonstrating stage-specific alterations in DNA synthesis in the TN3 and TN4 stages of thymocyte development as measured by BrdU incorporation after TCDD exposure (Laiosa et al., 2003). Moreover, given the striking functional and developmental differences that exist within the defined stages of thymocyte development, it was anticipated that our approach might reveal subtle yet critical differences in AHR-dependent gene regulation in a stage-specific manner. Specifically, we anticipated the possibility of detecting differences in AHR regulated gene expression between the T-cell–committed TN3 and TN4 stages, compared with the non–T-cell-committed TN1+2 stages of thymocyte development.

In support of our approach, we identified a number of genes that have been implicated as targets of AHR activation. Specifically, Cyp1a1, Cyp1b1, Lgals3, and the AHR repressor have all previously been identified in a number of cell types to be induced after exposure to AHR agonists (Mimura et al., 1999; Okey et al., 2005; Puga et al., 2005). In addition, we found that TCDD exposure led to the induction of *scinderin* and *KLF2*, two genes previously identified as AHR-dependent hematopoietic targets in the thymus (Svensson and Lundberg, 2001; Svensson et al., 2002; McMillan et al., 2007). The elevated thymus expression of scinderin after AHR activation identifies this protein as an interesting candidate potentially involved in mediating TCDD-induced changes in T-cell development and cell cycle regulation. Indeed, loss of scinderin expression has been associated with megakaryoblastic leukemia cells, and the forced expression of scinderin within these oncogenic cells dramatically reduced cell proliferation (Zunino et al., 2001). The decrease in the megakaryocyte proliferation was attributed, at least in part, to a loss of filamentous actin, which is important for cell division (Zunino et al., 2001). Given this potential cell-cycle regulatory role of scinderin, the earlier identification and our confirmation of scinderin expression in immature thymocytes after AHR activation raises the hypothesis that AHR activation in stage TN3 and TN4 thymocytes induces scinderin, leading to a decrease in filamentous actin and a rapid loss of cell proliferation.

Although confirmation of gene products previously shown to be induced by TCDD in the thymus provided confidence that our approach and methods were valid, new insights into potential mechanisms of AHR-dependent changes in T-cell development might be obtained from the identification of gene expression changes in a stage-specific manner. Indeed, our analysis resulted in the identification of seven gene products the expression of which varied only slightly in the TN1+2 subset but underwent significant modulation in the TN3, TN4A, and/or TN4B subset. Moreover, all seven gene probes reflected a decrease in gene expression in the appropriate populations. The decrease in gene expression after AHR activation, although not unprecedented, is generally not considered to be the primary mode by which AHR agonists affect transcriptional regulation (Gasiewicz et al., 2008).

Several possibilities exist as to why seven of the modulated genes from our gene profiling analysis are modulated in a stage-specific manner and why all of these genes show a decrease in expression levels. First, and perhaps most obvious, is that the AHR is directly involved in active repression

TABLE 3
IPA analysis of genes significantly modulated by AHR activation

Top IPA Associated Functional Networks	Score
Endocrine system development and function, lipid metabolism, small molecule biochemistry	43
Endocrine system development and function, small molecule biochemistry, drug metabolism	28
Lipid metabolism, small molecule biochemistry, cellular movement	27
Dermatological diseases and conditions, genetic disorder, immunological disease	22
Cell morphology, cellular development, cellular growth and proliferation	20

TABLE 4
IPA analysis of genes associated with biological functions significantly modulated by AHR activation

Top IPA Bio Functions	*P* Value Range	No. of Genes
Diseases and disorders		
Cancer	1.26×10^{-5}–3.49×10^{-2}	35
Hematological disease	6.08×10^{-5}–3.49×10^{-2}	17
Inflammatory response	2.28×10^{-4}–2.49×10^{-2}	14
Immunological disease	3.25×10^{-4}–3.49×10^{-2}	16
Gastrointestinal disease	1.35×10^{-3}–3.49×10^{-2}	6
Molecular and cellular functions		
Cellular growth and proliferation	3.01×10^{-6}–3.45×10^{-2}	29
Lipid metabolism	1.53×10^{-5}–3.11×10^{-2}	6
Small molecule biochemistry	1.53×10^{-5}–3.11×10^{-2}	15
Drug metabolism	4.59×10^{-5}–1.57×10^{-2}	3
Cellular development	9.03×10^{-5}–3.45×10^{-2}	21
Physiological system development and function		
Hematological system development and function	1.77×10^{-6}–3.49×10^{-2}	21
Tissue morphology	1.77×10^{-6}–2.73×10^{-2}	16
Tumor morphology	1.26×10^{-5}–2.73×10^{-2}	10
Endocrine system development and function	1.53×10^{-5}–3.11×10^{-2}	3
Respiratory system development and function	1.52×10^{-4}–3.94×10^{-3}	2

TABLE 5
IPA analysis of genes associated with canonical pathways significantly modulated by AHR activation

Top IPA Canonical Pathways	*P*	Ratio
Aryl hydrocarbon receptor signaling	1.76×10^{-4}	5/155 (0.032)
Xenobiotic metabolism signaling	1.91×10^{-4}	6/254 (0.024)
Virus entry via endocytic pathways	2.96×10^{-4}	4/96 (0.042)
Glucocorticoid receptor signaling	3.33×10^{-4}	6/278 (0.022)
PPARα/RXRα activation	3.92×10^{-4}	5/185 (0.027)

PPAR, peroxisome proliferator-activated receptor; RXR, retinoid X receptor.

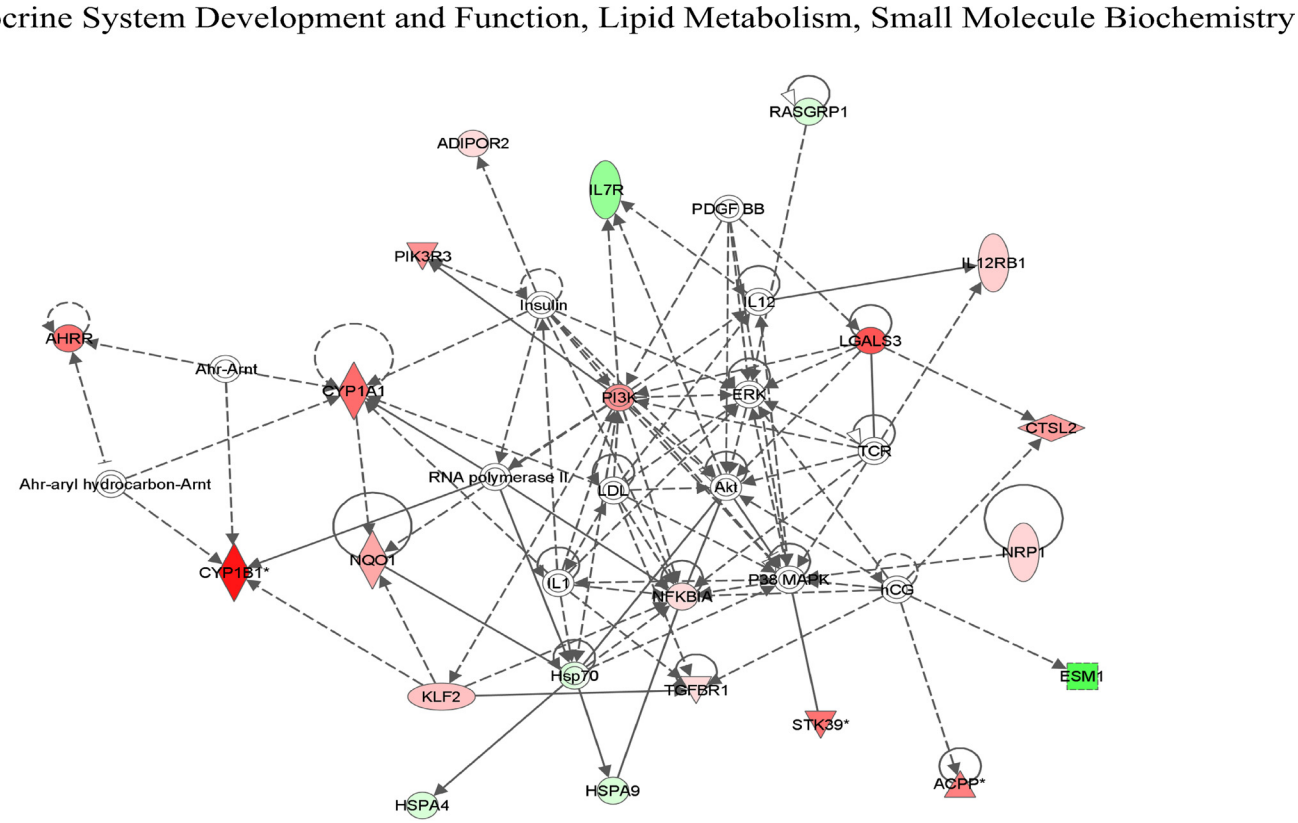

Fig. 5. Top implicated biological networks containing genes significantly changed by TCDD exposure. Expression values are overlaid in green (decreased) or red (increased). For conventions and symbols, refer to Ingenuity website legend description (https://analysis.ingenuity.com/pa/info/help/help.htm#legend.htm).

of these genes through recognition of AHREs present in the upstream regions of the genes. Indeed, all seven genes had at least one core AHRE consensus sequence (GCGTG), and Pprc1, Tmem97, and Wdr12 also possess extended AHRE consensus sequences (TNGCGTG) in their enhancer regions (data not shown). Alternatively, the AHR may act indirectly on the transcription of these seven genes by inducing repressor protein(s) involved in turning off their expression. In addition, the TN3 stage of thymocyte development is the developmental stage at which TCRβ rearrangement and pre-TCR–dependent signals drive $\alpha\beta$ T-cell commitment. Thus, there may be factors intrinsic to stages TN3–TN4 (including but not limited to the pre-TCR complex, for example) that coordinate with AHR-dependent signal transduction to modulate genes controlling growth and developmental processes.

Indeed, five of the seven genes in which expression was decreased in stages TN3–TN4 have been associated with cell growth and proliferation processes. Of these genes, decreased expression in four of the five is consistent with a block in progression through the cell cycle. Specifically, 5-methythioadenosine phosphorylase (Mtap) is a critical enzyme required for the salvage pathway for methionine and adenine biosynthesis (Avila et al., 2004). In the absence of Mtap, the precursor product methylthioadenosine (Mta) accumulates; Mta has been demonstrated to inhibit cell proliferation in some cellular systems (Avila et al., 2004). It is odd that loss of Mtap has also been associated with several types of tumors; however, excess Mta is thought to be secreted by these abnormal cells (Avila et al., 2004). Although decreased Mtap expression within stage TN3–TN4 thymocytes could potentially account for the observed decrease in DNA synthesis observed in these cells, the kinetics of its loss would seem to suggest it is not the primary candidate. Moreover, gene expression levels of Mtap do not decline significantly until the 12-h time point, concurrent with the time when BrdU incorporation is also inhibited. Thus, although Mtap deficiency and Mta accumulation may contribute to the observed cell cycle defects, the kinetics are inconsistent with a causative relationship.

Compared with Mtap, expression of Pprc1, Tmem97, and Wdr12 are all attenuated at the 6-h time point in at least one of the three T-cell-committed subpopulations (TN3, TN4A, and TN4B). Of these, Tmem97 (also known as Mac30) and Wdr12 have been implicated in cellular processes affecting cellular growth and proliferation. Specifically, Wdr12 is a critical member of a three-protein nucleolar protein complex known as a PeBoW complex (Rohrmoser et al., 2007). Knockdown experiments demonstrate that disruptions to the formation of the complex result in a failure to make the 28S rRNA, resulting in a p53-dependent cell cycle arrest (Rohrmoser et al., 2007). Tmem97 expression, in contrast, is associated with several different human tumors and has been implicated as a possible oncogene (Moparthi et al., 2007). However, Tmem97 has also been implicated in cholesterol/lipid biosynthetic pathways (Wilcox et al., 2007). Thus, an improved understanding of the putative function of Tmem97 is required before a definitive role in mediating AhR-dependent changes in T-cell development can be concluded. Nevertheless, the kinetics and magnitude by which its expression levels are attenuated within the TN3 compartment suggest further study may be warranted.

In addition to identification of potential cell-cycle regulatory genes, our analysis revealed modulation of the immune specific genes *IL-7R*, and *TGFβR1*. Specifically, elevation of TGFβR1 expression by TCDD in stages TN1+2, TN3, and TN4A may increase the sensitivity of these cells to members of the TGFβ superfamily that signal at least in part through TGFβR1, including TGFβ1, TGFβ2, bone morphogen proteins, and activins. Collectively, TGFβ superfamily proteins are known to both positively and negatively modulate early thymocyte development; however, the mechanism by which the appropriate balance is maintained is an area of active investigation (Licona-Limón and Soldevila, 2007). Thus, a model system in which the receptor expression levels are affected by AHR activation during early thymocyte development might be useful for dissecting the contribution of TGFβ superfamily proteins during thymocyte development. In addition, TGFβ is well established as an AHR-dependent target in many other studies suggesting an important AHR-dependent regulatory loop with potential influence during thymocyte development. It is noteworthy that the absence of a significant induction of TGFβ at 6 and 12 h after TCDD exposure in the present study suggests that TGFβ production is cell-, tissue-, and/or time-dependent.

In contrast to TGFβR1, IL-7R expression is attenuated by TCDD during the TN1+2 and TN3 stages of development, potentially decreasing the sensitivity of these cells to IL-7. IL-7 is normally associated with cell survival and maturation just before TCRβ selection (Petrie and Zúñiga-Pflücker, 2007). Thus, the attenuation of IL-7 receptor levels by TCDD suggested by the current study may result in fewer cells receiving the appropriate maturational signals required for pre-TCR–dependent cell proliferation during the TN3-to-TN4 transition. Taken together, the subtle effects of AHR modulation on IL7R and TGFβR1 levels observed in our study may offer clues as to how the AHR potentially tunes early thymocyte development in response to normal intrinsic microenvironmental signals.

Of course, speculation about the potential role individual AHR-dependent gene targets may play in modulating early thymocyte development and cell proliferation fails to acknowledge the broad network of gene targets being modulated that ultimately contribute to the observed phenotype. To gain a broader understanding of the cellular and molecular pathways modulated by AHR activation, we employed the ingenuity pathway assist. Indeed, the top molecular and cellular functions modulated in the early thymocyte progenitor compartment belong to cell growth and proliferation family with the association of 29 of 108 gene probes. Moreover, genes associated with oncological, hematological, immunological, and inflammatory diseases were enriched in our gene profiling experiment, suggesting that understanding the role of the activated AHR during early thymocyte development may provide insight and potentially novel therapeutic approaches for these immune diseases.

In this gene-profiling experiment, we have shown for the first time that within the same immunological tissue, AHR activation by TCDD modulates gene expression differently depending on the stage of thymocyte differentiation. The gene expression fingerprint within T-cell-committed stages of thymocyte development in which TCDD was previously shown to affect cell cycle regulation (TN3, TN4A, and TN4B), is uniquely different from the TN1+2 stages in which cell cycle regulation is largely unaffected and cells are still uncommitted to the $\alpha\beta$ T-cell lineage. The specificity of these

gene changes both temporally and in TN3 and TN4 supports the notion that the AHR has an intrinsic developmental role at this stage of thymocyte ontogeny. Functional networks associated with cell growth, proliferation, and cellular development are clearly modulated by AHR activation within early thymocyte progenitors. This finding is consistent with the rapid and dramatic decrease in cell proliferation previously observed in these stages of thymocyte development after exposure to TCDD. However, more work is needed to dissect how and why proper regulation of the AHR is so important at these thymocyte progenitor stages and how the AHR plays such a critical role in determining the ultimate function of T cells. Finally, the observed differences in the AHR-modulated gene expression fingerprint revealed within different developmental stages in the thymus may have implications for other tissues where AHR signal transduction seems to be functionally important.

Acknowledgments

We thank Dr. Nicholas Gonchoroff (Upstate Medical University Flow Cytometry Core) for expert advice and Karen Gentile (Upstate Medical University, Microarray Core) for technical assistance with microarray analysis.

References

Avila MA, García-Trevijano ER, Lu SC, Corrales FJ, and Mato JM (2004) Methylthioadenosine. *Int J Biochem Cell Biol* **36:**2125–2130.

Fernandez-Salguero PM, Hilbert DM, Rudikoff S, Ward JM, and Gonzalez FJ (1996) Aryl-hydrocarbon receptor-deficient mice are resistant to 2,3,7,8-tetrachlorodibenzo-p-dioxin-induced toxicity. *Toxicol Appl Pharmacol* **140:**173–179.

Funatake CJ, Marshall NB, Steppan LB, Mourich DV, and Kerkvliet NI (2005) Cutting edge: activation of the aryl hydrocarbon receptor by 2,3,7,8-tetrachlorodibenzo-p-dioxin generates a population of CD4+ CD25+ cells with characteristics of regulatory T cells. *J Immunol* **175:**4184–4188.

Garrett RW and Gasiewicz TA (2006) The aryl hydrocarbon receptor agonist 2,3,7,8-tetrachlorodibenzo-p-dioxin alters the circadian rhythms, quiescence, and expression of clock genes in murine hematopoietic stem and progenitor cells. *Mol Pharmacol* **69:**2076–2083.

Gasiewicz TA, Henry EC, and Collins LL (2008) Expression and activity of aryl hydrocarbon receptors in development and cancer. *Crit Rev Eukaryot Gene Expr* **18:**279–321.

Hogaboam JP, Moore AJ, and Lawrence BP (2008) The aryl hydrocarbon receptor affects distinct tissue compartments during ontogeny of the immune system. *Toxicol Sci* **102:**160–170.

Laiosa MD, Wyman A, Murante FG, Fiore NC, Staples JE, Gasiewicz TA, and Silverstone AE (2003) Cell proliferation arrest within intrathymic lymphocyte progenitor cells causes thymic atrophy mediated by the aryl hydrocarbon receptor. *J Immunol* **171:**4582–4591.

Levelt CN, Mombaerts P, Iglesias A, Tonegawa S, and Eichmann K (1993) Restoration of early thymocyte differentiation in T-cell receptor beta-chain-deficient mutant mice by transmembrane signaling through CD3 epsilon. *Proc Natl Acad Sci USA* **90:**11401–11405.

Licona-Limón P and Soldevila G (2007) The role of TGF-beta superfamily during T cell development: new insights. *Immunol Lett* **109:**1–12.

McMillan BJ, McMillan SN, Glover E, and Bradfield CA (2007) 2,3,7,8-Tetrachlorodibenzo-p-dioxin induces premature activation of the KLF2 regulon during thymocyte development. *J Biol Chem* **282:**12590–12597.

Mimura J, Ema M, Sogawa K, and Fujii-Kuriyama Y (1999) Identification of a novel mechanism of regulation of Ah (dioxin) receptor function. *Genes Dev* **13:**20–25.

Mombaerts P, Iacomini J, Johnson RS, Herrup K, Tonegawa S, and Papaioannou VE (1992) RAG-1-deficient mice have no mature B and T lymphocytes. *Cell* **68:**869–877.

Moparthi SB, Arbman G, Wallin A, Kayed H, Kleeff J, Zentgraf H, and Sun XF (2007) Expression of MAC30 protein is related to survival and biological variables in primary and metastatic colorectal cancers. *Int J Oncol* **30:**91–95.

Okey AB, Franc MA, Moffat ID, Tijet N, Boutros PC, Korkalainen M, Tuomisto J, and Pohjanvirta R (2005) Toxicological implications of polymorphisms in receptors for xenobiotic chemicals: the case of the aryl hydrocarbon receptor. *Toxicol Appl Pharmacol* **207 (2 Suppl):**43–51.

Petrie HT and Zúñiga-Pflücker JC (2007) Zoned out: functional mapping of stromal signaling microenvironments in the thymus. *Annu Rev Immunol* **25:**649–679.

Puga A, Tomlinson CR, and Xia Y (2005) Ah receptor signals cross-talk with multiple developmental pathways. *Biochem Pharmacol* **69:**199–207.

Quintana FJ, Basso AS, Iglesias AH, Korn T, Farez MF, Bettelli E, Caccamo M, Oukka M, and Weiner HL (2008) Control of T(reg) and T(H)17 cell differentiation by the aryl hydrocarbon receptor. *Nature* **453:**65–71.

Rohrmoser M, Hölzel M, Grimm T, Malamoussi A, Harasim T, Orban M, Pfisterer I, Gruber-Eber A, Kremmer E, and Eick D (2007) Interdependence of Pes1, Bop1, and WDR12 controls nucleolar localization and assembly of the PeBoW complex required for maturation of the 60S ribosomal subunit. *Mol Cell Biol* **27:**3682–3694.

Schmidt JV, Su GH, Reddy JK, Simon MC, and Bradfield CA (1996) Characterization of a murine Ahr-null allele: involvement of the Ah receptor in hepatic growth and development. *Proc Natl Acad Sci USA* **93:**6731–6736.

Stevens EA, Mezrich JD, and Bradfield CA (2009) The aryl hydrocarbon receptor: a perspective on potential roles in the immune system. *Immunology* **127:**299–311.

Stockinger B, Veldhoen M, and Hirota K (2009) Modulation of Th17 development and function by activation of the aryl hydrocarbon receptor—the role of endogenous ligands. *Eur J Immunol* **39:**652–654.

Svensson C and Lundberg K (2001) Immune-specific up-regulation of adseverin gene expression by 2,3,7,8-tetrachlorodibenzo-p-dioxin. *Mol Pharmacol* **60:**135–142.

Svensson C, Silverstone AE, Lai ZW, and Lundberg K (2002) Dioxin-induced adseverin expression in the mouse thymus is strictly regulated and dependent on the aryl hydrocarbon receptor. *Biochem Biophys Res Commun* **291:**1194–1200.

Veldhoen M, Hirota K, Westendorf AM, Buer J, Dumoutier L, Renauld JC, and Stockinger B (2008) The aryl hydrocarbon receptor links TH17-cell-mediated autoimmunity to environmental toxins. *Nature* **453:**106–109.

Wilcox CB, Feddes GO, Willett-Brozick JE, Hsu LC, DeLoia JA, and Baysal BE (2007) Coordinate up-regulation of TMEM97 and cholesterol biosynthesis genes in normal ovarian surface epithelial cells treated with progesterone: implications for pathogenesis of ovarian cancer. *BMC Cancer* **7:**223.

Zunino R, Li Q, Rosé SD, Romero-Benítez MM, Lejen T, Brandan NC, and Trifaró JM (2001) Expression of scinderin in megakaryoblastic leukemia cells induces differentiation, maturation, and apoptosis with release of plateletlike particles and inhibits proliferation and tumorigenesis. *Blood* **98:**2210–2219.

Address correspondence to: Dr. Michael D. Laiosa, University of Wisconsin-Milwaukee School of Public Health, 3209 North Maryland Avenue, Milwaukee, WI 53211. E-mail: laiosa@uwm.ed